

1 **Persistence of populations facing climate velocity and**
2 **harvest**

3 Emma Fuller¹, Eleanor Brush², Malin L. Pinsky^{1,3}

4 (1): Department of Ecology and Evolutionary Biology, Princeton University, Princeton, New
5 Jersey 08544 USA

6 (2): Program in Quantitative and Computational Biology, Princeton University, Princeton, New
7 Jersey 08544 USA

8 (3): Department of Ecology, Evolution and Natural Resources, Rutgers University, New
9 Brunswick, New Jersey 08901 USA

10 **Abstract**

11 Many species are expected to shift their geographic distribution as climates change, and yet
12 climate change is only one of a suite of stressors that species face. Species that might, in theory,
13 be able to shift rapidly enough to keep up with climate velocity (the rate and direction that
14 isotherms move across the landscape) may not in actuality be able to do so when facing the
15 cumulative impacts of multiple stressors. However, despite empirical reports of substantial
16 interactions between climate change and other stressors, we often lack a mechanistic
17 understanding of these interactions. Here, we develop and analyze a spatial population dynamics
18 model to explore the cumulative impacts of climate with another dominant stressor in the ocean
19 and on land: harvest. Our results delineate the conditions under which harvesting and climate
20 velocity can together drive populations extinct even when neither stressor would do so in
21 isolation. We find that critical rates of harvest and climate velocity depend on the growth rate
22 and dispersal kernel of the population, as well as the magnitude of the other stressor. We also
23 find that, in our model, the declines in biomass caused by climate velocity and harvest are at
24 most slightly greater than the sum of the declines caused by either stressor individually (e.g.,
25 approximately additive) and that threshold harvest rules and protected areas can be effective
26 management tools to mitigate the interaction between the two stressors.

27 **Keywords:** Climate change, fishing, integrodifference model, synergy, multiple disturbances,
28 cumulative impacts

29 **Introduction**

30 There are many stressors that can disturb an ecosystem, and ecologists have long quantified the
31 consequences of individual perturbations (Wilcove et al. 1998). Less work, however, has been
32 done to measure the effects of multiple stressors and the interactions between them (Travis 2003;
33 Crain et al. 2008; Darling and Côté 2008). If disturbances interact synergistically, a perturbation
34 that has little effect when occurring alone may amplify the disturbance caused by a coincident
35 perturbation (Crain et al. 2008; Darling and Côté 2008; Nye et al. 2013; Gurevitch et al. 2000).
36 In the most worrying cases, interactions among multiple stressors could drive a population
37 extinct even though assessments of individual impacts would suggest otherwise (e.g., Pelletier et
38 al. 2006; Travis 2003). Because disturbances rarely occur in isolation, measuring the effects of
39 multiple disturbances provides a better understanding of likely impacts to an ecosystem (Doak
40 and Morris 2010; Fordham et al. 2013; Folt et al. 1999).

41 Climate change and harvesting, two of the largest anthropogenic impacts for both marine and
42 terrestrial species (Milner-Gulland and Bennet 2003; Sekercioglu et al. 2008; Halpern et al.
43 2008), provide an important example of ecological disturbances occurring in unison. One effect
44 of climate change is that isotherms move across a landscape with a rate and direction referred to
45 as climate velocity (Loarie et al. 2009; Burrows et al. 2011). Marine and terrestrial population
46 distributions shift in response to climate change (Perry et al. 2005; Chen et al. 2011), and there is
47 evidence that climate velocities can successfully explain these shifts (Pinsky et al. 2013).

48 Many of these shifting species, however, are also subject to harvesting or fishing (Wilcove et al.
49 1998; Sala 2000; Worm et al. 2009), and there is therefore great potential for interactions
50 between the two stressors. For example, empirical data suggest that Atlantic croaker populations

51 move poleward with warming temperatures, but do so less when heavily fished (Hare et al.
52 2010). In addition, climate and fishing both appear to have influenced the distribution of North
53 Sea cod over the past century (Engelhard et al. 2014). While not specifically addressing range
54 shifts and harvest together, synergistic interactions between warming temperatures and
55 harvesting have been identified in microcosm experiments (Mora et al. 2007), observations
56 suggest that species follow warming temperatures more effectively in protected areas than in
57 unprotected land (Thomas et al. 2012), and a number of studies conclude that harvest increases
58 the sensitivity of populations to climate variability (Anderson et al. 2008; Botsford et al. 2011;
59 Shelton et al. 2011; Planque et al. 2011). Taken together, this work underscores the importance
60 of understanding in greater mechanistic detail how climate velocity and harvesting interact.
61 Models provide a useful tool in this situation for building our intuition.

62 A common approach to modeling climate impacts has been to use bioclimatic-envelope models
63 (also known as species distribution models). These statistical models typically correlate
64 presence-absence or abundance data with biophysical characteristics to predict how species'
65 ranges will differ under climate change (Elith et al. 2006; Guisan and Thuiller 2005; Guisan and
66 Zimmermann 2000). Despite these models' widespread adoption, many authors have criticized
67 bioclimatic-envelope models as oversimplified because they lack dispersal, reproduction, species
68 interaction, and other processes important for population dynamics (Kearney and Porter 2009;
69 Zarnetske et al. 2012; Robinson et al. 2011).

70 Recent work on range shifts has addressed some of these gaps by explicitly including dispersal
71 and reproduction in models for species distributions under climate change (Berestycki et al.
72 2009; Zhou and Kot 2011). In these latter models, the region in which a population can survive
73 (e.g., the region of suitable temperatures) is shifting in space, and a population can only survive

74 if it disperses to and grows in newly suitable habitat at a sufficient rate. Related models have
75 been applied to study population persistence in advective environments (Byers and Pringle
76 2006). However, even these more mechanistic models only address one disturbance: climate-
77 driven range shifts.

78 Here, we focus on a relatively simple ecological model that captures the dominant processes
79 (reproduction, dispersal, and population growth) underlying climate-driven range shifts and
80 population responses to harvesting pressure. We built this model originally for marine species;
81 but because of its mathematical generality, it could also apply to any species with distinct growth
82 and dispersal stages (e.g., plants, trees, and many insects). We derive the harvesting rate and
83 climate velocity that drive populations extinct, and explore the combined demographic effects of
84 these stressors. We show that the declines in biomass caused by climate-driven range shifts and
85 harvest are at most only slightly greater than the sum of the declines caused by either stressor
86 individually. In other words, the cumulative impacts are approximately additive. Finally, we
87 examine the efficacy of two different types of management strategies: threshold harvesting rules
88 and protected areas. Protected areas are often recommended for conservation of biodiversity and
89 improved yield from harvest (Pimm et al. 2001, Gaines et al. 2010b, Watson et al. 2011), and
90 previous work has suggested protected areas can be a key form of climate insurance that
91 provides stepping stones to help species keep up with a changing environment (Thomas et al.
92 2012; Hannah et al. 2007). We find that protected areas can help a species persist with higher
93 harvesting pressure and can increase the maximum climate velocity a harvested species can
94 survive. However, in our model, threshold-harvesting rules have a fundamentally different effect
95 and largely remove one of the strongest interactions between harvesting rates and climate
96 velocity.

97 **Methods**

98 We model the dynamics of populations along a one-dimensional line of longitude, similar to
99 Zhou and Kot (2011). Individuals in the population can only reproduce within a defined segment
100 of the environment (hereafter simply “patch”), which represents the range of thermally suitable
101 conditions for the population. The patch shifts at a fixed rate towards the poles (i.e., at the rate of
102 climate velocity), and offspring disperse away from their parents according to a dispersal kernel.
103 In its basic form, harvest removes a constant fraction of the local population density from each
104 point along the coastline.

105 To investigate the model, we first analytically determine the combinations of harvesting rate and
106 climate velocity that drive the population extinct (hereafter the critical harvesting rate and critical
107 climate velocity), and then measure their interaction by calculating the decrease in biomass
108 caused by the stressors both individually and together. We then add threshold harvesting rules
109 and protected areas in numerical simulations to determine how these management strategies
110 affect population persistence and biomass.

111 **The Model**

112 The above verbal description is represented well by integro-difference models, which have been
113 used extensively for spatial population dynamics problems with discrete time (e.g., discrete
114 growth and dispersal stages) and continuous space (Kot and Schaffer 1996; Van Kirk and Lewis
115 1997; Lockwood et al. 2002; Zhou and Kot 2010). More specifically, if $n_t(x)$ is the number of
116 individuals settling after dispersal at position x and time t , then the number of individuals in the
117 next generation is given by

$$n_{t+1}(x) = \int_{-\frac{L}{2}+ct}^{\frac{L}{2}+ct} k(x-y)R_0g(f(n_t(y))) dy, \quad (1)$$

118 where $f(n)$ is a recruitment function describing the number of offspring that settle and survive in
 119 juvenile population of size n , $g(n)$ is a function describing the number of adults that remain after
 120 harvesting given local density $n_t(y)$, R_0 is the intrinsic growth rate of the population (e.g.,
 121 number of offspring per adult), $k(x - y)$, is a dispersal kernel giving the probability of an
 122 offspring traveling from position y to position x . The model integrates over all reproduction that
 123 occurs within the suitable thermal habitat patch, where L is the length of the patch and c is the
 124 rate at which the patch shifts across space (the rate of climate velocity). In other words, the
 125 center of the patch at time t will be at location ct , and so the upper and lower bounds of the
 126 patch will be found at $ct + L/2$ and $ct - L/2$.

127 Initially, we use $g(n) = n - hn$ as our function for those surviving harvesting, where h is the
 128 proportion of the population harvested. This model envisions that harvest removes a constant
 129 fraction from each location x , as could be expected from an even distribution of harvesters across
 130 space.

131 We also used a Beverton-Holt stock-recruitment function to describe the settlement and survival
 132 of offspring $f(n)$ accounting for density dependent competition and mortality:

$$f(n_t) = \frac{n_t}{1 + \left(\frac{R_0-1}{K}\right)n_t} \quad (2)$$

133 As before, R_0 is the intrinsic growth rate, while K is the carrying capacity at a given point in
 134 space, which we assume to be constant (see Table 1 for a full description of parameters and

135 functions). If $n_t = K$, then $f(n_t) = \frac{n_t}{R_0}$ and when those surviving offspring reproduce at rate R_0
 136 the population will remain at K . As shown in Appendix A.1, the precise forms of $g(n)$ and $f(n)$
 137 are not important to the persistence of the population, which instead depends only on $g'(0)$ and
 138 $f'(0)$. The full functional forms, however, are important for equilibrium population levels.

139 Analyzing this kind of model becomes easier if the dispersal kernel is separable into its
 140 dependence on sources and destinations of larvae, that is if there are functions a_i, b_i such that
 141 $k(x - y) = \sum_{i=1}^{\infty} a_i(x)b_i(y)$ (see Appendix A.2 for further details). In the analyses presented
 142 below, we used a Gaussian kernel (Latore et al. 1998) given by

$$k(x - y) = \frac{1}{2\sqrt{D\pi}} e^{\frac{-(x-y)^2}{4D}}. \quad (3)$$

143 To derive analytical expressions for the critical rates of harvesting and climate velocity, we
 144 approximate the kernel to its first-order terms, as described in Appendix A.3. Further, to examine
 145 the sensitivity of the model to the shape of the kernel, we also analyze a sinusoidal kernel (see
 146 Appendix A.4).

147 At demographic equilibrium, the population will move in a traveling wave, where the population
 148 density at a given point in space will change, but the density at a location relative to the shifting
 149 patch will not (Zhou and Kot 2011). The traveling wave n^* must satisfy

$$n^*(\bar{x}) = \int_{-\frac{L}{2}}^{\frac{L}{2}} k(\bar{x} + c - \bar{y}) R_0(1 - h) f(n^*(\bar{y})) d\bar{y}, \quad (4)$$

150 where $\bar{x}, \bar{y} \in \left[-\frac{L}{2}, \frac{L}{2}\right]$ describes the position within the patch. For a separable kernel, the
 151 equilibrium traveling pulse $n^*(x)$ must satisfy

$$n^*(x) = \sum_{i=1}^{\infty} a_i(x) \int_{-\frac{L}{2}}^{\frac{L}{2}} b_i(y - c) R_0(1 - h) f(n^*(y)) dy = \sum_{i=1}^{\infty} m_i a_i(x), \quad (5)$$

152 where the m_i satisfy the equations

$$m_i = \int_{-\frac{L}{2}}^{\frac{L}{2}} b_i(y - c) R_0(1 - h) f\left(\sum_{j=1}^{\infty} m_j a_j(y)\right) dy \quad (6)$$

153 (Latore et al. 1998). We show the derivation of these equations in Appendix A.2.

154 Persistence

155 At low harvesting rates h and low climate velocities c , marine populations will persist. However,
 156 above certain critical values, populations will be driven extinct. When the population is extinct,
 157 the system is in its trivial equilibrium; $n^*(\bar{x}) = 0$ for all $x \in \left[-\frac{L}{2}, \frac{L}{2}\right]$, which satisfies Equation 4.

158 If a population is to persist, it must be able to avoid extinction and grow even when small (Zhou
 159 and Kot 2011). Population persistence is therefore equivalent to the trivial traveling pulse being
 160 an unstable equilibrium, where the introduction of a small population will grow rather than
 161 return to extinction. The critical parameters h^* and c^* are defined as the parameters that make the
 162 trivial pulse unstable. See Appendix A.1 for further details of this analytical calculation.

163 Regardless of the functional form of the recruitment function f , its only property that determines
 164 whether or not a population can persist is how quickly recruitment increases when the population
 165 size is near (but above) 0. For us, this number is 1, and any recruitment function with the same
 166 value will give the same results with respect to persistence. Therefore, the population's ability to
 167 persist depends on properties of the population itself (the intrinsic growth rate R_0 , the shape of
 168 the dispersal kernel, and the expected distance a larva disperses $\langle d \rangle$), properties of the

169 environment (the length of the viable patch L and how quickly the environment shifts c), and the
170 harvesting rate h . For a Gaussian kernel, the critical rates c^* and h^* are those values of c and h
171 such that

$$R_0(1-h)2\sqrt{2}\exp\left(\frac{-c^2}{8D}\right)\left[\operatorname{erf}\left(\frac{L-c}{2\sqrt{2D}}\right)-\operatorname{erf}\left(\frac{-L-c}{2\sqrt{2D}}\right)\right]=1. \quad (7)$$

172

173 We derive a similar expression for a sinusoidal kernel in the Appendix A.4. We realize that this
174 formula is not straightforward to understand. For both Gaussian and sinusoidal kernels, however,
175 we can approximate the critical harvesting proportion by a function that looks like

$$h^* \sim 1 - \frac{1}{R_0} \cdot p(L, R_0)q(\langle d \rangle, c^2, L^2 + 3c^2), \quad (8)$$

176

177 where p is a decreasing function of the length of the viable patch and the intrinsic growth rate,
178 and q describes how h^* increases with patch length (L) and varies with expected dispersal
179 distance and climate velocity (see Appendix A.5 for details).

180 **Calculating the interaction of climate velocity and harvest**

181 In order to quantify how harvesting interacts with climate velocity, we find the total biomass of
182 the population when it reaches an equilibrium traveling pulse and compare this equilibrium
183 biomass in the presence and absence of each stressor individually or the two stressors together.
184 Equations 5 and 6 allow us to numerically find the total biomass in the equilibrium traveling
185 pulse under each of these conditions.

186 We use B_0 to denote the equilibrium biomass without either stressor, B_h the equilibrium biomass
187 with harvesting but with climate velocity equal to 0, B_c the equilibrium biomass with climate
188 velocity greater than 0 but no harvesting, and B_{hc} the equilibrium biomass with both stressors.
189 For each stressor or combination of stressors, we calculate the decline in biomass caused by
190 stressor s as

$$E_s = B_0 - B_s. \quad (9)$$

191
192 Based upon this definition, there are three kinds of interaction types that can be defined. If the
193 interaction is purely additive, then the cumulative response to both stressors together would be
194 $E_{hc} = E_h + E_c$. If the stressors instead interact synergistically, then $E_{hc} > E_h + E_c$. In contrast, the
195 stressors would interact antagonistically if $E_{hc} < E_h + E_c$.

196 We can quantify the degree of synergy as

$$S = E_{hc} - (E_h + E_c). \quad (10)$$

197 where positive S indicates synergy, negative S indicates antagonism, and S of zero indicates
198 purely additive interactions. This is a common way to measure the interaction among stressors,
199 though alternative approaches can use the ratio of affected to unaffected biomass as a measure of
200 effect size (multiplicative model) or consider the effect of the single worst stressor (simple
201 comparative effects model) (Folt et al. 1999; Crain et al. 2008). The additive model is the most
202 conservative when quantifying negative effects, as we do here, meaning that it is less likely to
203 identify synergistic interactions (Folt et al. 2012; Crain et al. 2008).

205 **Simulations**

206 We use simulations to implement two management strategies (threshold harvesting rules and
207 protected areas) that make our basic integrodifference model analytically intractable. Under
208 threshold harvesting, harvesting pressure was no longer implemented as a proportional removal
209 from the population. Instead, we evaluate the abundance at each point in space to determine how
210 much harvesting should occur. If the population abundance is below the designated threshold, no
211 harvesting occurs. If the population exceeded the threshold, then we harvest all the ‘surplus’
212 individuals. This approach is an extreme version of the harvest control rules proposed for many
213 existing fisheries (Froese et al. 2011).

214 In addition, we introduce networks of protected areas into our simulations by designating
215 segments of space where the harvesting rate was equal to 0. Protected areas, particularly in the
216 ocean, are typically designed to meet either harvest management or conservation goals (Agardy
217 1994; Holland and Brazee 1996; Gaines et al. 2010a), thus their spacing and size differ. Harvest-
218 oriented protected areas are often designed such that they maximize adult spillover into
219 harvestable areas by creating many small reserves closely spaced (Hastings and Botsford 2003;
220 Gaylord et al. 2005; Gaines et al. 2010a). To mimic this management scheme, we implemented
221 protected areas with a length 1/3 of the average dispersal distance and an inter-reserve spacing
222 2/3 of the average dispersal distance. Conservation-oriented protected areas seek to protect
223 entire ecosystems and reduce adult spillover by creating fewer, larger protected areas (Toonen et
224 al. 2013). To mimic this scheme, we implement protected areas with a length 4 times the average
225 dispersal distance and an inter-reserve spacing 8 times the average dispersal distance between
226 them (Lockwood et al. 2002). In both harvest-oriented and conservation-oriented protected area
227 networks, 1/3 of the coastline is protected. With protected areas present we either assume that

228 harvesting is proportional in areas between reserves or that harvesting pressure remains constant,
229 and is shifted to available, unprotected habitat.

230 For every simulation, we seed the model with 50 individuals at a single location and iterate for
231 2000 generations to reach equilibrium without harvesting or climate shift (more than sufficient
232 based on initial tests). We then add harvesting pressure, allow the population to again reach
233 equilibrium (2000 generations), and finally add a changing climate by moving the viable patch
234 with a certain velocity. After 6000 generations we calculate equilibrium biomass as the mean
235 biomass of 2000 additional generations. Implementing protected areas makes the population
236 abundance cycle, averaging over 2000 generations is sufficient to erase effects of periodicity in
237 results. If population abundance declines below 0.001, the population is considered extinct (i.e.
238 abundance is 0). For all simulations, we use a Laplace dispersal kernel, $k(x - y) = \frac{1}{2}be^{-b|x-y|}$,
239 which is a commonly used model of marine larval dispersal (Botsford et al. 2001) that, however,
240 is not amenable to the analytical methods we use above.

241 **Results**

242 **Persistence with Harvesting and Climate Velocity**

243 We begin by examining the critical rates of harvesting and climate velocity, i.e., those rates
244 sufficient to drive a population extinct. As would be expected, we find that the critical rate of
245 each stressor is lower if a population faces higher intensities of the other stressor (downward
246 curving lines in Figure 1). For example, a harvesting rate that is sustainable in the absence of
247 environmental shift (c near zero) may no longer be sustainable if the environment begins to
248 change rapidly ($c \gg$ zero).

249 We also examine the sensitivity of critical rates to growth and dispersal. In our model, it is
250 always the case that increasing the intrinsic growth rate (R_0), all else being equal, will increase
251 the critical climate velocity c^* and the critical harvesting rate h^* , since a population that grows
252 more quickly can recover more effectively from losses caused by these stressors (compare lines
253 with different shading in Figure 1). However, whether or not dispersing farther is better depends
254 on how quickly the environment is shifting (compare solid and dashed lines in Figure 1). When
255 the environment is shifting slowly, populations with wider dispersal kernels have a lower critical
256 harvesting rate because dispersing farther results in too many larvae dispersing off the viable
257 patch. When the environment is shifting quickly, on the other hand, populations with wider
258 dispersal kernels can better withstand harvesting because larvae dispersing long distances more
259 effectively colonize the habitat patch that will be viable in the next generation.

260 **Interactions Between Stressors**

261 It is also important to ask how a population responds to moderate cumulative impacts that are
262 insufficient to drive it extinct. Whenever climate velocity or harvesting pressure exceeds their
263 critical rate, the biomass of the population at equilibrium will be equal to 0 (the definition of the
264 critical rate). Before the stressors reach those thresholds, however, the equilibrium biomass of
265 the population decreases smoothly as either the harvesting pressure or the rate of environmental
266 shift increases (Figure 2a).

267 When we compare the cumulative impacts of the stressors to the sum of each stressor
268 individually we find low levels of positive synergy between the two stressors (Figure 2b). The
269 stressors display a synergistic interaction most strongly at high harvest and climate velocity rates,
270 close to where they would drive the population extinct. As a note, positive synergy indicates that

271 cumulative impacts cause the population to lose more biomass than we would predict from either
272 stressor individually. However, the degree of synergy is low and concentrated in a limited part of
273 parameter space. Throughout much of the range of harvest rates and climate velocities, the
274 interaction between the stressors is quite close to an additive model. Results are robust to
275 changes from a Gaussian to a sinusoidal dispersal kernel.

276 **Alternative management strategies**

277 Under a constant harvest rate, we find that harvest rate and climate velocity interact such that
278 more heavily harvested populations go extinct with slower climate velocities. However, with
279 harvest thresholds in place, a small population can always escape harvesting and the critical
280 climate velocity c^* no longer depends on the harvesting rate (Figure 3b). In other words, as long
281 as there is some threshold population density below which harvesting is not allowed, critical
282 climate velocity in our model only depends on the growth rate, length of the viable patch, and
283 average dispersal distance. In this case, the interaction follows a simple comparative model, such
284 that the cumulative impacts of the two stressors are equal to the individual effect of the worst
285 stressor.

286 With either type of protected area strategies in effect (many small versus few large), the
287 population withstands combinations of higher climate velocities and higher harvesting rates than
288 without the protected areas (compare Figures 3c and d to Figure 3a). However, there are also
289 some differences between the large and the small protected area strategies. At lower climate
290 velocities, protected areas spaced more than one average dispersal distance apart result in larger
291 fluctuations of population biomass relative to small, closely spaced protected areas (Appendix
292 A.6, Figure S1). Minimum population biomass is higher in simulations with smaller protected

293 areas, potentially providing a larger buffer against extinction relative to simulations with larger
294 but more widely spaced protected areas.

295 **Discussion**

296 Climate change and harvest are two of the dominant human impacts on marine species and many
297 terrestrial species, but our understanding for their joint effects and interactions remains limited.
298 By analyzing a general model that incorporates dispersal and reproduction, we show that climate
299 velocity and harvesting interact strongly in their effects on species persistence and biomass. In
300 particular, we find that the critical harvesting rate decreases as climate velocity increases. In
301 other words, the more quickly the environment shifts, the less harvesting it takes to drive the
302 population extinct. The interaction between climate velocity and harvesting are additive for most
303 combinations of stressor levels, with weak synergy only appearing close to population extinction.
304 However, harvesting rules that avoid harvest from low-density parts of the population, such as
305 the leading edge, change the interaction substantially. In the latter case, the population only
306 decreases by an amount equal to the effect of the single worst stressor (whether climate velocity
307 or harvest).

308 Our results suggest that particular combinations of harvesting and climate velocity will affect
309 certain species more than others. Species with a higher intrinsic population growth rate (i.e.,
310 growth rate at low abundance) and a longer average dispersal distance will better track rapid
311 climate velocities, as compared to species with a low intrinsic population growth rate and short
312 dispersal distances. This finding matches previous expectations: higher growth rates make a
313 population more resistant to the removals from harvesting or the losses associated with tracking
314 climate velocity. It is worth pointing out that a higher population growth rates can be generated

315 either by shorter generation times or higher fecundity. Empirical work also suggests that marine
316 fish and invertebrates with faster life histories, as well as terrestrial birds and plants with greater
317 dispersal abilities, shifted their distributions more quickly in response to warming (Perry et al.
318 2005; Angert et al. 2011; Pinsky et al. 2013).

319 While higher reproductive rates improve a population's ability to persist in our model, higher
320 dispersal distances did not necessarily do so. In agreement with related results from Zhou and
321 Kot (2011), we found that at low speeds, a short dispersal distance improved the maximum
322 harvesting rate a population could sustain, while at higher speeds a longer dispersal distance
323 improved the maximum climate velocity under which the population could persist. It appears that
324 climate velocity could selectively favor species with dispersal distances best matched to the rate
325 of shift.

326 One goal of our model is to examine the cumulative impacts of multiple stressors. We find that
327 the interaction between harvest and climate velocity is effectively additive, with weak synergistic
328 effects appearing primarily when the population is close to extinction. This result from our
329 model would appear to contrast with other demonstrations of synergy between harvest and
330 climate in the literature. For example, a number of modeling and empirical studies have found
331 that fishing increases the sensitivity of populations to climate variability (including Anderson et
332 al. 2008; Shelton et al. 2011; Botsford et al. 2011), and a recent review reaches the same
333 conclusion (Planque et al. 2010). Positive feedback loops involving the loss of predators due to
334 fishing have also been identified that amplify climate impacts on prey species (Kirby et al. 2009;
335 Planque et al. 2010; Ling et al. 2009). Similarly, synergy between harvesting and temperature
336 was detected in experimental populations of rotifers (Mora et al. 2007).

337 A partial explanation for the differences between our model results and the previous evidence for
338 synergy may be that we analyze the ability of populations to keep pace with climate velocity,
339 while many previous studies examined other aspects of changing climate. In the rotifer
340 experiment, for example, populations were subjected to warming temperatures, but organisms
341 were unable to relocate to thermal optima (Mora et al. 2007). In many other fishing and climate
342 studies, the impacts of climate variability on stationary populations have been the focus, rather
343 than cumulative climate change or shifting distributions (Walters and Parma 1996; Anderson et
344 al. 2008; Shelton et al. 2011; Botsford et al. 2011; Planque et al. 2010). Work that does
345 incorporate shifting species distributions typically examines regional or global scenarios for
346 climate change, making it difficult to isolate the effect that different species interactions, climate
347 and harvesting each play (Cheung et al. 2010).

348 Another explanation for the discrepancy may be that the only effect of harvesting in our model is
349 a reduction in the size of the adult biomass. In reality, populations often contain a diversity of
350 subpopulations, ages, and genotypes that can buffer them against climate variability and climate
351 change (Schindler et al. 2010). Harvest tends to simplify this diversity within populations,
352 making them more sensitive to climate variability (Mora et al. 2007; Planque et al. 2010). Our
353 model also did not include food web dynamics or species interactions, although some positive
354 feedback loops and synergistic interactions identified between climate and harvesting in previous
355 studies involved the loss of predators and the release of prey (Kirby et al. 2009; Ling et al. 2009).
356 Our simple, single-species, non-age-structured model suggests that additive interactions between
357 climate velocity and harvesting constitute a reasonable baseline or “null” expectation in the
358 absence of more complicated mechanisms. Future work considering food web processes and

359 genetic, spatial, and age diversity will be important to examine other possible sources of
360 synergistic (or antagonistic) interactions between harvesting and climate velocity.

361 We also examine whether two frequently recommended management approaches, protected
362 areas and harvest control rules, could help ensure species persistence in the face of multiple
363 stressors. With either of these management strategies, we generally find increases in the
364 population's biomass at equilibrium and an improved ability to persist. Threshold harvesting
365 rules in particular appear to fundamentally alter much of the interaction between the two
366 stressors. In our model, thresholds appear to have this effect because they effectively prevent
367 harvesting of the leading edge and allow colonization to occur as if these individuals were
368 moving into un-harvested areas. This result matches well with invasion theory, which has shown
369 that populations move into new territory at a rate approximately equal to $2\sqrt{R_0 l}$, where l is the
370 mean squared displacement of individuals per unit time (Fisher 1937). With a constant harvest
371 rate applied everywhere, the invasion rate drops to $2\sqrt{(1 - h)R_0 l}$, whereas the invasion rate is
372 unaffected if harvesting avoids the leading edge. It's interesting to note that novel, low
373 abundance stocks are commonly unregulated in fisheries systems (Beddington et al. 2007;
374 Dowling et al. 2008). Whether fisheries and other harvesting activities rapidly exploit newly
375 colonizing species depends in part on the interaction of social, economic, and regulatory factors
376 (Pinsky and Fogarty 2012). Our work, however, highlights the fact that a low (or zero) harvest
377 rate on species that have recently colonized new habitats can be important for helping them keep
378 up with rapid climate velocities.

379 Unlike thresholds, protected areas are spatially explicit. Previous work has advanced protected
380 areas as a way to help organisms keep pace with shifting climates, as well as to ameliorate

381 anthropogenic disturbances like harvesting and habitat fragmentation (Lawler et al. 2010;
382 Hannah et al. 2007; Botsford et al. 2001; Gaylord et al. 2005; Hastings and Botsford 2003;
383 Thomas et al. 2012, Watson et al. 2011). Our results show that protected areas increase the
384 equilibrium biomass of harvested populations at a given climate velocity, which supports their
385 use as a tool to help these populations withstand the effects of climate velocity. However, the
386 details of protected-area design affect our results: few, large protected areas increase population
387 fluctuations at low climate velocities, while many smaller protected areas maintain a population
388 bounded farther from extinction. This effect appears because large gaps separate our large
389 protected areas, which allows harvest to drive populations to lower levels while between
390 protected areas. In contrast, populations were less fully exposed to harvesting while traversing
391 the smaller gaps between small protected areas. While the discussion of many small vs. few large
392 protected areas involves many factors (Gaines et al. 2010b; McCarthy et al. 2011), our results
393 contribute to this body of work by showing that small gaps between protected areas, even if
394 counter-balanced by small protected areas, may help species keep up with climate velocities in
395 the face of harvest.

396 The advantage of a simple model like ours is that it is potentially general enough to apply to a
397 wide range of species. Our discrete-time, continuous-space model captures the processes
398 important to species with distinct growth and dispersal stages, including most marine organisms,
399 plants, trees, and many insects. Our approach does not capture all the complexities of real
400 populations or of harvesting dynamics, however. For example, we do not include the potential
401 for negative per capita growth at low densities, often called Allee or depensation effects.
402 Invasion theory suggests that Allee effects generally have two impacts: they slow initial rates of
403 spread, and they allow predation to, in some cases, slow or stop an invasion (Hastings et al.

404 2005). Based on first principles, we would expect similar effects in a model like ours, suggesting
405 that populations with Allee effects will be more sensitive to the combined effects of harvest and
406 climate velocity than our model initially suggests. We also did not include age structure or other
407 aspects of sub-population diversity (e.g., spatial or genetic) in our model. As described above,
408 these forms of diversity have been important for studying the joint effects of harvesting and
409 climate variability (Botsford et al. 2011; Planque et al. 2010), and will likely be important for
410 understanding climate velocity impacts as well. Besides these species-specific extensions, this
411 modeling framework could also be extended to consider species interactions, such as between
412 predator and prey (Gilman et al. 2010). A final important extension is better capturing harvesting
413 dynamics. We find that the distribution of harvesting pressure affects the outcomes of our simple
414 model (i.e. thresholds, versus proportional harvesting). Harvester behavior, to the extent it has
415 been considered in fisheries, highlights considerable uncertainty in how vessels allocate effort
416 over space and respond to changes in environmental conditions (Fulton et al. 2011, Van Putten et
417 al. 2011, Pinsky and Fogarty 2012). These responses are rarely integrated into modeling
418 efforts, and an important next step is integrated assessments of social-ecological systems.

419 Using a simple, mechanistic model like the one we present here helps to build intuition about the
420 conditions under which species can survive the cumulative impacts of climate and harvesting.
421 This work highlights the importance of considering stressors in combination, as outcomes
422 deviate from what we would predict in isolation. It also shows the importance of alternative
423 management strategies, as the location of harvest greatly affects the interaction between
424 harvesting and climate. While management strategies only change harvesting practices and do
425 not directly address climate change, understanding how management approaches can affect
426 interactions between harvesting and range shifts will help to improve harvesting rules and the

427 development of protected areas. Our results are encouraging evidence that management practices
428 can help protect marine populations from the cumulative impacts of harvesting and climate
429 change.

430 Acknowledgements

431 We thank Catherine Offord and Will Scott for discussions on this project, and James Watson,
432 Emily Klein and Simon Levin for comments on an earlier draft. EF acknowledges support from
433 the National Science Foundation (GRFP, GEO-1211972), EB acknowledges support from the
434 National Institute of Health (NIH 5T32HG003284), and MP acknowledges support from a David
435 H. Smith Conservation Research Fellowship.

436 Literature Cited

- 437 Agardy, M. Tundi. 1994. Advances in marine conservation: the role of marine protected areas.
438 *Trends in Ecology & Evolution* 9: 267–270.
- 439 Anderson, C.N.K., et al. 2008. Why fishing magnifies fluctuations in fish abundance. *Nature*
440 452: 835–9.
- 441 Angert, A.L., L. G. Crozier, L. J. Rissler, S. E. Gilman, J. J. Tewksbury and A. J. Chunco, 2011.
442 Do species' traits predict recent shifts at expanding range edges? *Ecology Letters* 14: 677–89.
- 443 Beddington, J.R., D. J. Agnew, and C. W. Clark. 2007. Current problems in the management of
444 marine fisheries. *Science* 316: 1713–6.
- 445 Berestycki, H., O. Diekmann, C. J. Nagelkerke, and P. A. Zegeling. 2009. Can a species keep
446 pace with a shifting climate? *Bulletin of Mathematical Biology* 71: 399–429.
- 447 Botsford, L. W., A. Hastings, and S. D. Gaines. 2001. Dependence of sustainability on the
448 configuration of marine reserves and larval dispersal distance. *Ecology Letters* 4: 144–150.
- 449 Botsford, L. W., M. D. Holland, J. F. Samhouri, J. W. White, and A. Hastings. 2011. Importance
450 of age structure in models of the response of upper trophic levels to fishing and climate change.
451 *ICES Journal of Marine Science: Journal du Conseil* 68: 1270–1283.

- 452 Burrows, M. T., et al. 2011. The pace of shifting climate in marine and terrestrial ecosystems.
453 *Science* 334: 652-5.
- 454 Byers, J. E. and J. M. Pringle. 2006. Going against the flow: retention, range limits and invasions
455 in advective environments. *Marine Ecology Progress Series* 313: 27-41.
- 456 Chen, I. C., J. K. Hill, R. Ohlemüller, D. B. Roy, and C. D. Thomas. 2011. Rapid range shifts of
457 species associated with high levels of climate warming. *Science* 333: 1024-6.
- 458 Cheung, W. W. L., V. W. Y. Lam, J. L. Sarmiento, K. Kearney, R. E. G. Watson, D. Zeller, and
459 D. Pauly. 2010. Large-scale redistribution of maximum fisheries catch potential in the global
460 ocean under climate change. *Global Change Biology* 16: 24–35.
- 461 Crain, C. M., K. Kroeker, and B. S. Halpern. 2008. Interactive and cumulative effects of multiple
462 human stressors in marine systems. *Ecology Letters* 11: 1304–15.
- 463 Darling, E. S., and I. M. Côté. 2008. Quantifying the evidence for ecological synergies. *Ecology*
464 *Letters* 11: 1278–86.
- 465 Doak, D. F., and W. F. Morris. 2010. Demographic compensation and tipping points in climate-
466 induced range shifts. *Nature* 467: 959–62.
- 467 Dowling, N. A., et al. 2008. Developing harvest strategies for low-value and data-poor fisheries:
468 Case studies from three Australian fisheries. *Fisheries Research* 94: 380–390.
- 469 Elith, J., et al. 2006. methods improve prediction of species' distributions from occurrence data.
470 *Ecography* 29: 129–151.
- 471 Engelhard, G.H., D. A. Righton, and J. K. Pinnegar. 2014. Climate change and fishing: a century
472 of shifting distribution in North Sea cod. *Global Change Biology*. doi: 10.1111/gcb.12513
- 473 Fisher, R.A. 1937. The wave of advance of advantageous genes. *Annals of Eugenics* 7: 355-369.
- 474 Folt, C. L., C. Y. Chen, M. V. Moore, and J. Burnaford. 1999. Synergism and antagonism among
475 multiple stressors. *Limnology and Oceanography* 44: 864–877.
- 476 Fordham, D. A. A., et al. 2013. Population dynamics can be more important than physiological
477 limits for determining range shifts under climate change. *Global Change Biology* 19: 3224-3237.
- 478 Froese, R., T. A. Branch, A. Proelß, M. Quaas, K. Sainsbury, and C. Zimmermann. 2011.
479 Generic harvest control rules for European fisheries. *Fish and Fisheries* 12: 340–351.
- 480 Fulton, E. A., A. D. M. Smith, D. C. Smith, D. C., and I. E. van Putten. 2011. Human behaviour:
481 The key source of uncertainty in fisheries management. *Fish and Fisheries*, 12: 2-17.
- 483 Gaines, S. D., C. White, M. H. Carr, and S. R. Palumbi. 2010a. Designing marine reserve
484 networks for both conservation and fisheries management. *Proceedings of the National Academy
485 of Sciences USA* 107: 18286–93.

- 486 Gaines, S. D., S. E. Lester, K. Grorud-Colvert, C. Costello, and R. Pollnac. 2010b. Evolving
487 science of marine reserves: new developments and emerging research frontiers. *Proceedings of*
488 *the National Academy of Sciences USA* 107: 18251–5.
- 489 Gaylord, B., S. D. Gaines, D. A. Siegel, and M. H. Carr. 2005. Marine reserves exploit
490 population structure and life history in potentially improving fisheries yields. *Ecological*
491 *Applications* 15: 2180–2191.
- 492 Gilman, S.E., M. C. Urban, J. J. Tewksbury, G. W. Gilchrist, and R. D. Holt. 2010. A framework
493 for community interactions under climate change. *Trends in Ecology and Evolution* 25: 325–331.
- 494 Guisan, A. and W. Thuiller. 2005. Predicting species distribution: offering more than simple
495 habitat models. *Ecology Letters* 8: 993–1009.
- 496 Guisan, A. and N. E. Zimmermann. 2000. Predictive habitat distribution models in ecology.
497 *Ecological modelling* 135: 147–186.
- 498 Gurevitch, J., J. A. Morrison, and L. V. Hedges. 2000. The Interaction between Competition and
499 Predation: A Metaanalysis of Field Experiments. *The American Naturalist* 155: 435–453.
- 500 Halpern, B. S., et al. 2008. A global map of human impact on marine ecosystems. *Science* 319:
501 948–52.
- 502 Hannah, L., G. Midgley, S. Andelman, M. Araújo, G. Hughes, E. Martinez-Meyer, R. Pearson,
503 and P. Williams. 2007. Protected area needs in a changing climate. *Frontiers in Ecology and the*
504 *Environment* 5: 131–138.
- 505 Hare, J.A., M. A. Alexander, M. J. Fogarty, E. H. Williams, and J. D. Scott. 2010. Forecasting
506 the dynamics of a coastal fishery species using a coupled climate-population model. *Ecological*
507 *Applications* 20: 452–64.
- 508 Hastings, A., et al. 2005. The spatial spread of invasions: new developments in theory and
509 evidence. *Ecology Letters* 8: 91–101.
- 510 Hastings, A. and L. W. Botsford. 2003. Comparing designs of marine reserves for fisheries and
511 for biodiversity. *Ecological Applications* 13: 65–70.
- 512 Holland, D. S., and R. J. Brazee. 1996. Marine reserves for fisheries management. *Marine*
513 *Resource Economics* 11: 157–172.
- 514 Kearney, M. and W. Porter. 2009. Mechanistic niche modelling: combining physiological and
515 spatial data to predict species' ranges. *Ecology Letters* 12: 334–50.
- 516 Kirby, R. R., G. Beaugrand, and J. A. Lindley. 2009. Synergistic Effects of Climate and Fishing
517 in a Marine Ecosystem. *Ecosystems* 12: 548–556.
- 518 Kot, M. and W. M. Schaffer. 1986. Discrete-time growth-dispersal models. *Mathematical*
519 *Biosciences* 80: 109–136.
- 520 Latore, J., P. Gould, and A. M. Mortimer. 1998. Spatial dynamics and critical patch size of
521 annual plant populations. *Journal of Theoretical Biology* 190: 277–285.

- 522 Lawler, J. J., et al. 2010. Resource management in a changing and uncertain climate. *Frontiers in*
523 *Ecology and the Environment* 8: 35–43.
- 524 Ling, S. D., C. R. Johnson, S. D. Frusher, and K. R. Ridgway. 2009. Overfishing reduces
525 resilience of kelp beds to climate-driven catastrophic phase shift. *Proceedings of the National*
526 *Academy of Sciences USA* 106: 22341–22345.
- 527 Loarie, S. R. P. B. Duffy, H. Hamilton, G. P. Asner, C. B. Field, and D. D. Ackerly. 2009. The
528 velocity of climate change. *Nature*, 462: 1052-5.
- 529 Lockwood, D. R., A. Hastings, and L. W. Botsford. 2002. The effects of dispersal patterns on
530 marine reserves: does the tail wag the dog? *Theoretical Population Biology* 61: 297–309.
- 531 McCarthy, M.A., C. J. Thompson, A. L. Moore, and H. P. Possingham. 2011. Designing nature
532 reserves in the face of uncertainty. *Ecology Letters* 14: 470–5.
- 533 Milner-Gulland, J., and E. L. Bennett. 2003. Wild meat: The bigger picture. *Trends in Ecology &*
534 *Evolution*, 18: 351-357.
- 535 Mora, C., R. Metzger, A. Rollo, and R. A. Myers. 2007. Experimental simulations about the
536 effects of overexploitation and habitat fragmentation on populations facing environmental
537 warming. *Proceedings of the Royal Society B* 274: 1023–1028.
- 538 Nye, J. A., R. J. Gamble, and J. S. Link. 2013. The relative impact of warming and removing top
539 predators on the Northeast US large marine biotic community. *Ecological Modelling* 264: 157–
540 168.
- 541 Pelletier, E., P. Sargian, J. Payet, and S. Demers. 2006. Ecotoxicological effects of combined
542 UVB and organic contaminants in coastal waters: a review. *Photochemistry and photobiology*
543 82: 981–993.
- 544 Perry, A. L., P. J. Low, J. R. Ellis, and J. D. Reynolds. 2005. Climate Change and Distribution
545 Shifts in Marine Fishes. *Science* 308: 1912–1915.
- 546 Pimm, S., et al. 2001. Can we defy nature's end? *Science*, 293: 2207-2208.
- 547 Pinsky, M. 2011. Dispersal, Fishing, and the Conservation of Marine Species. Stanford
548 University: Stanford University.
- 549 Pinsky, M. L., and M. Fogarty. 2012. Lagged social-ecological responses to climate and range
550 shifts in fisheries. *Climatic Change* 115: 883-891.
- 551 Pinsky, M. L., B. Worm, M. J. Fogarty, J. L. Sarmiento, and S. A. Levin. 2013. Marine taxa
552 track local climate velocities. *Science* 341: 1239-42.
- 553 Planque, B., J. Fromentin, P. Cury, K. F. Drinkwater, S. Jennings, R. I. Perry, and S. Kifani.
554 2010. How does fishing alter marine populations and ecosystems sensitivity to climate? *Journal*
555 *of Marine Systems* 79: 403–417.
- 556 Robinson, L. M. M., J. Elith, A. J. J. Hobday, R. G. G. Pearson, B. E. E. Kendall, H. P. P.
557 Possingham, and A. J. J. Richardson. 2011. Pushing the limits in marine species distribution

- 558 modelling: lessons from the land present challenges and opportunities. *Global Ecology and*
559 *Biogeography* 20: 789–802.
- 560 Schindler, D.E., et al. 2010. Population diversity and the portfolio effect in an exploited species.
561 *Nature* 465: 609–12.
- 562 Sala, O. E. E., et al. 2000. Global biodiversity scenarios for the year 2100. *Science* 287: 1770–
563 1774.
- 564 Sekercioglu, C. H., S. H. Schneider, J. P. Fay, and S. R. Loarie. 2008. Climate Change,
565 Elevational Range Shifts, and Bird Extinctions. *Conservation Biology* 22: 140-150.
- 566 Shelton, A.O. and M. Mangel. 2011. Fluctuations of fish populations and the magnifying effects
567 of fishing. *Proceedings National Academy Sciences USA* 108: 7075–7080.
- 568 Thomas, C. D., et al. 2012. Protected areas facilitate species' range expansions. *Proceedings of*
569 *the National Academy of Sciences USA* 109: 14063–8.
- 570 Toonen, R.J., et al. (2013). One size does not fit all: the emerging frontier in large-scale marine
571 conservation. *Marine Pollution Bulletin* 77: 7–10.
- 572
- 573 Travis, J. M. J.. 2003. Climate change and habitat destruction: a deadly anthropogenic cocktail.
574 *Proceedings of the Royal Society B: Biological Sciences* 270 (1514): 467-73.
- 575 Van Kirk, R. W. and M. A. Lewis. 1997. Integrodifference models for persistence in fragmented
576 habitats. *Bulletin of Mathematical Biology* 59: 107–137.
- 577 van Putten, I. E., S. Kulmala, O. Thébaud, N. Dowling, K. G. Hamon, T. Hutton, and S. Pascoe.
578 2011. Theories and behavioural drivers underlying fleet dynamics models. *Fish and Fisheries*
579 13: 216-235.
- 580 Walters, C., and A. M. Parma. 1996. Fixed exploitation rate strategies for coping with effects of
581 climate change. *Canadian Journal of Fisheries and Aquatic Sciences* 53: 148–158.
- 582 Watson, J. R., D. A. Siegel, B. E. Kendall, S. Mitarai, A. Rassweiller, and S. D. Gaines. 2011.
583 Identifying critical regions in small-world marine metapopulations. *Proceedings of the National
584 Academy of Sciences USA* 108: e907-e913.
- 585 Wilcove, D. S., D. R., J. Dubow, A. Phillips, and E. Losos. 1998. Quantifying threats to
586 imperiled species in the United States. *BioScience* 48: 607–615.
- 587 Worm, B., et al. 2009. Rebuilding global fisheries. *Science* 325: 578-585.
- 588 Zarnetske, P. L., D. K. Skelly, and M. C. Urban. 2012. Ecology. Biotic multipliers of climate
589 change. *Science* 336: 1516–8.
- 590 Zhou, Y., and M. Kot. 2011. Discrete-time growth-dispersal models with shifting species ranges.
591 *Theoretical Ecology* 4: 13–25.
- 592

593 **Tables**

594 **Table 1: Parameter values and functions used in the text**

Variable	Definition
$n_t(x)$	density of individuals at position x at time t
$n^*(\bar{x})$	density of individuals at equilibrium at position \bar{x} relative to the patch
$k(x - y)$	dispersal kernel, the probability of offspring traveling from position y to position x
$\langle d \rangle$	expected distance traveled by an offspring
$f(n)$	recruitment function, the number of offspring produced by a population of size n
R_0	intrinsic growth rate of the population at low abundance
$g(n)$	harvest function, the number of adults remaining after a population of size n has been harvested
h	proportion of adults harvested, when $g(n) = hn$
L	patch length
c	climate velocity in units of distance per time

595

596 **Figure Legends**
597

598 Figure 1: (a) Lines indicate the critical threshold for persistence as a function of harvesting rate
599 on the y-axis and climate velocity on the x-axis. Shade of grey corresponds to the growth rate
600 from smallest to greatest (light to dark). Line style indicates the average dispersal distance (solid:
601 $\langle d \rangle = 0.1$ vs. dashed: $\langle d \rangle = 0.5$) from an approximated Gaussian dispersal kernel (Eq. 3). Patch
602 length $L = 1$.

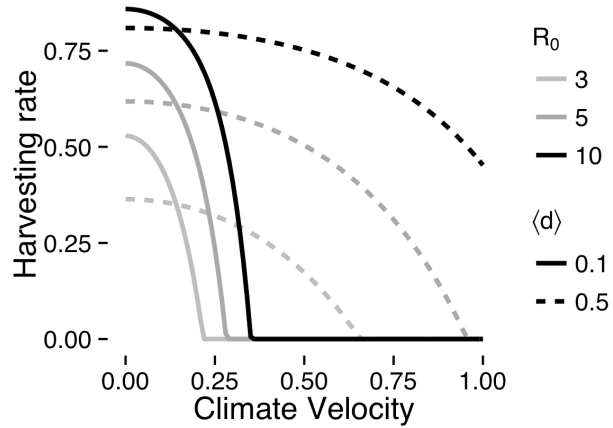
603 Figure 2: (a) The equilibrium biomass of the population as a function of the climate velocity on
604 the x-axis and the proportional harvesting rate on the y-axis. Results are from an approximated
605 Gaussian dispersal kernel with parameters $L = 1$, $R_0 = 10$, and $\langle d \rangle = 0.5$. (b) Interaction
606 between the two stressors as a function of climate velocity and harvesting rate. Shading indicates
607 the degree of synergistic interaction, i.e., the loss in biomass in the doubly stressed population in
608 excess of the sum of the losses caused by each stressor individually ($E_{hc} - E_h - E_c$). Synergy of
609 0 indicates additive interaction of the stressors. The excess loss, on the order of 0.001, is small in
610 comparison to the total biomass, which can be as large as 20. These results are from calculations
611 with the same parameters as Figure 2a.

612 Figure 3: The equilibrium biomass of the population as a function of the climate velocity on the
613 x-axis and the harvesting rate on the y-axis under alternative management strategies. (a) The
614 equilibrium biomass for simulations with constant harvest rates (compare to figure 2a). (b)
615 Equilibrium biomass for simulations with threshold management. For threshold management, the
616 maximum threshold is set to be the largest population size observed at a given time step before
617 harvesting. The y-axis is the proportion of the maximum threshold that is protected from
618 harvesting. (c) Equilibrium biomass for simulations with many small protected areas. (d)
619 Equilibrium biomass for simulations with few large protected areas. These results are from a
620 simulation with a Laplacian dispersal kernel with parameters $L = 1$, $R_0 = 5$, $K = 100$, and
621 $\langle d \rangle = 2$.

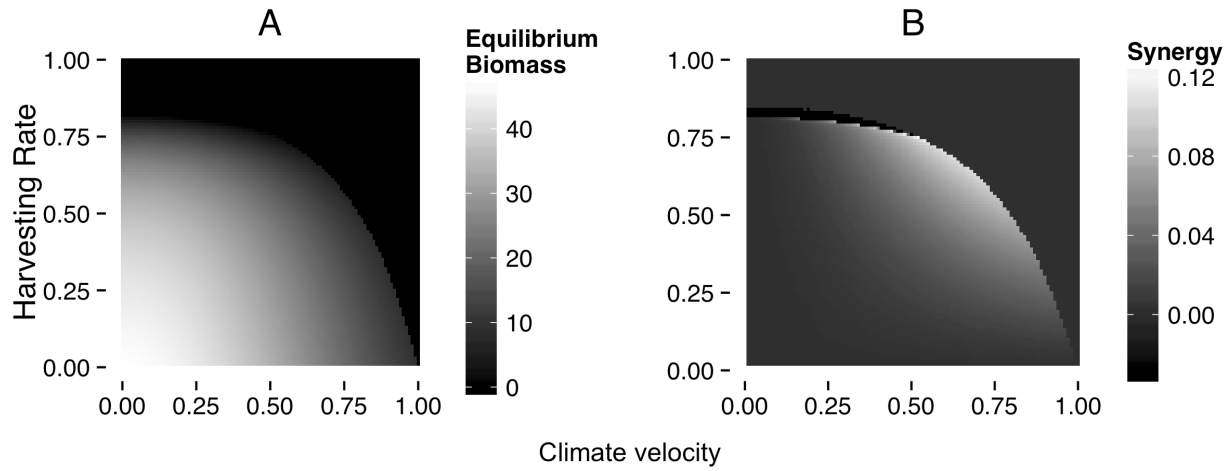
622

623 **Figures**

624

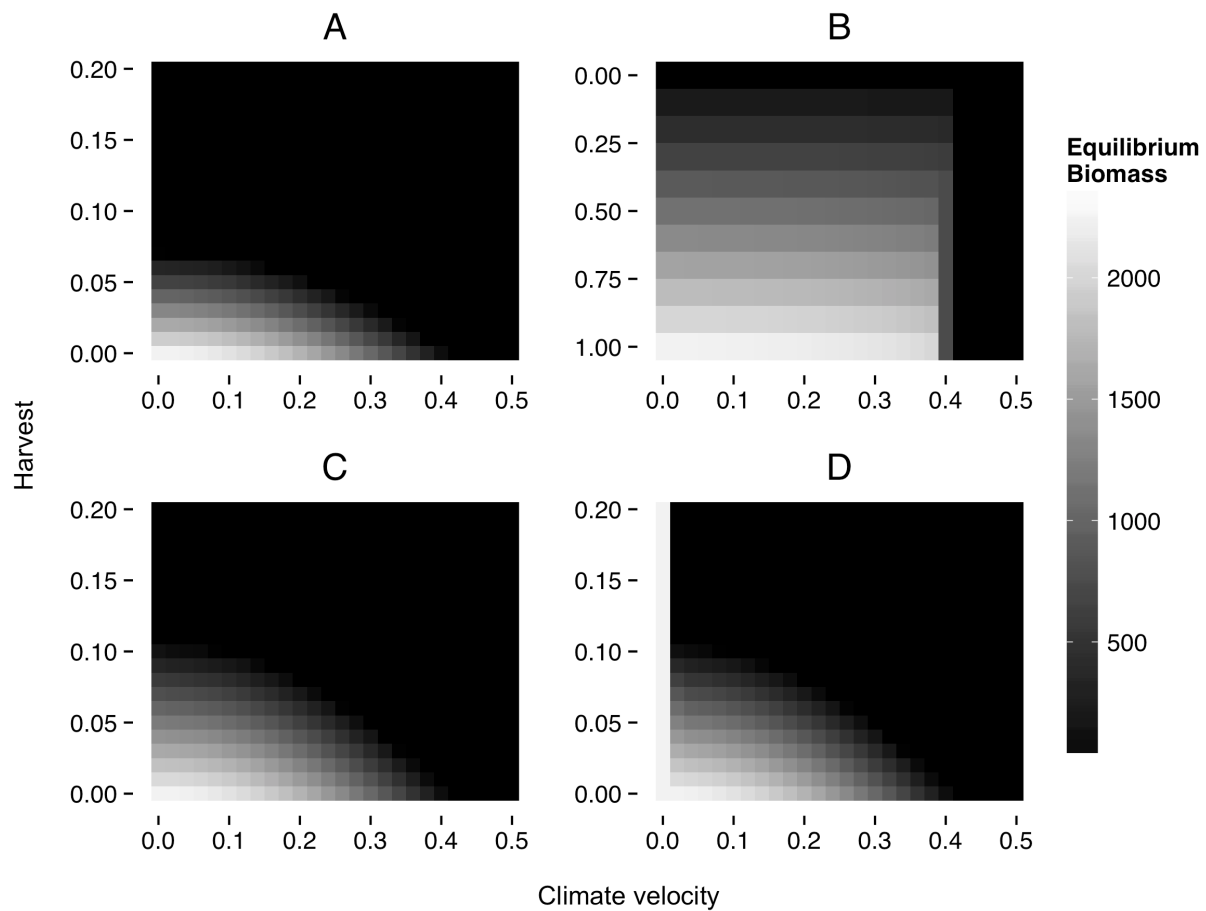


625 Figure 1



626

627 Figure 2



628

629 Figure 3

A Appendix

In Appendix A.1, we provide the details for assessing the persistence of a population with an integrodifference model and we discuss the effect of the harvesting function on population persistence. In Appendix A.2, we provide the details for assessing population persistence with separable dispersal kernels. In Appendix A.3 and A.4, we derive expressions for the critical harvesting rate and rate of environmental shift for Gaussian and sinusoidal dispersal kernels. In Appendix A.5, we derive approximate expressions for these critical rates. In Appendix A.6 we provide details on differences between small and large MPA simulations.

A.1 Determining stability Let $n_t(x)$ be the number of adults at position x at time t , let $k(x)$ be a dispersal kernel describing the probability of a larva traveling a distance x , let $f(n)$ be the recruitment function describing the number of offspring produced by a population of size n , and let $g(n)$ be the harvesting function describing the number of adults harvested from a population of size n . In the absence of harvesting, the integrodifference model describing the population over time is given by

$$n_{t+1}(x) = \int_{-L/2+ct}^{L/2+ct} k(x-y) R_0 f(n_t(y)) dy \quad (1)$$

as described in Zhou and Kot [2011]. With the addition of harvesting, the model becomes

$$n_{t+1}(x) = \int_{-L/2+ct}^{L/2+ct} k(x-y) R_0 g(f(n_t(y))) dy. \quad (2)$$

In evaluating persistence, we apply the methods of Zhou and Kot [2011] to the new model, Equation 2. A traveling pulse is a solution such that population size relative to location within the patch (rather than absolute position) is constant over time, i.e.

$$n^*(\bar{x}_t) \equiv n^*(x - ct) = n_t(x),$$

where $\bar{x}_t \equiv x - ct$ gives position relative to the patch.

The integrodifference equation (2) gives us an expression for n^* :

$$\begin{aligned} n^*(\bar{x}_{t+1}) &= n_{t+1}(x) \\ &= \int_{-L/2+ct}^{L/2+ct} k(x-y) R_0 g(f(n_t(y))) dy \\ &= \int_{-L/2+ct}^{L/2+ct} k(x - \bar{y}_t - ct) R_0 g(f(n^*(\bar{y}_t))) dy \\ &= \int_{-L/2+ct}^{L/2+ct} k(\bar{x}_t - \bar{y}_t) R_0 g(f(n^*(\bar{y}_t))) dy \\ \Rightarrow n^*(\bar{x}_t - c) &= \int_{-L/2+ct}^{L/2+ct} k(\bar{x}_t - \bar{y}_t) R_0 g(f(n^*(\bar{y}_t))) dy \\ \Rightarrow n^*(\bar{x}_t) &= \int_{-L/2}^{L/2} k(\bar{x}_t + c - \bar{y}_t) R_0 g(f(n^*(\bar{y}_t))) d\bar{y}_t \end{aligned} \quad (3)$$

As long as $f(0) = 0$, there is a trivial solution to this problem where $n^*(\bar{x}) \equiv 0$ for all \bar{x} , i.e., there is a trivial traveling pulse with no fish in it. If the trivial traveling pulse is unstable, even very small populations will persist or grow and avoid crashing back to the trivial pulse. To evaluate the stability of a traveling pulse, we introduce a small perturbation to the traveling pulse $n^*(\bar{x})$ and see if this perturbation grows or shrinks over time:

$$\begin{aligned}
n_t(x) &= n^*(\bar{x}_t) + \xi_t(x) \\
\Rightarrow \xi_{t+1}(x) &= n_{t+1}(x) - n^*(\bar{x}_{t+1}) \\
&= n_{t+1}(x) - n^*(\bar{x}_t - c) \\
&= \int_{-L/2+ct}^{L/2+ct} k(x-y) R_0 g(f(n_t(y))) dy - \int_{-L/2}^{L/2} k(\bar{x}_t - \bar{y}_t) R_0 g(f(n^*(\bar{y}_t))) d\bar{y}_t \text{ using (3)} \\
&= \int_{-L/2+ct}^{L/2+ct} k(x-y) R_0 g(f(n_t(y))) dy - \int_{-L/2+ct}^{L/2+ct} k(x-ct-(y-ct)) R_0 g(f(n^*(\bar{y}_t))) d\bar{y}_t \\
&= \int_{-L/2+ct}^{L/2+ct} k(x-y) R_0 g(f(n_t(y))) dy - \int_{-L/2+ct}^{L/2+ct} k(x-y) R_0 g(f(n^*(\bar{y}_t))) d\bar{y}_t \\
&= \int_{-L/2+ct}^{L/2+ct} k(x-y) \left(R_0 g(f(n_t(y))) - R_0 g(f(n^*(\bar{y}_t))) \right) dy \\
&= \int_{-L/2+ct}^{L/2+ct} k(x-y) R_0 \left(g(f(n_t(y))) - g(f(n^*(\bar{y}_t))) \right) dy \\
\Rightarrow \xi_{t+1}(x) &= \int_{-L/2+ct}^{L/2+ct} k(x-y) R_0 g'(f(n^*(\bar{y}))) f'(n^*(\bar{y})) (n_t(y) - n^*(\bar{y}_t)) dy \\
&\quad \text{by linearizing around the traveling pulse} \\
\Rightarrow \xi_{t+1}(x) &= \int_{-L/2+ct}^{L/2+ct} k(x-y) R_0 g'(f(n^*(\bar{y}))) f'(n^*(\bar{y})) \xi_t(y) dy \\
\Rightarrow \xi_{t+1}(x) &= \int_{-L/2+ct}^{L/2+ct} k(x-y) R_0 g'(0) f'(0) \xi_t(y) dy \text{ if } n^*(\bar{x}) = 0 \text{ and } f(0) = 0 \tag{4}
\end{aligned}$$

If we assume $\xi_t(x) = \lambda^t u(x-ct)$ for some $\lambda \in \mathbb{R}$ and $u : [-L/2, L/2] \rightarrow \mathbb{R}$, then the perturbation grows in time if and only if $\lambda > 1$. Using Equation (4), we can rewrite $\xi_{t+1}(x)$,

$$\begin{aligned}
\lambda u(x-ct-c) &= R_0 g'(0) f'(0) \int_{-L/2+ct}^{L/2+ct} k(x-y) u(y-ct) dy \\
\Rightarrow \lambda u(\bar{x}) &= R_0 g'(0) f'(0) \int_{-L/2}^{L/2} k(\bar{x}+c-\bar{y}) u(\bar{y}) dy
\end{aligned}$$

Define the integral operator

$$\psi_f(u)(x) = R_0 g'(0) f'(0) \int_{-L/2}^{L/2} k(x+c-y) u(y) dy.$$

Then the perturbation to the traveling pulse will satisfy

$$\psi_f(u)(x) = \lambda u(x) \tag{5}$$

λ and u are thus an eigenvalue and eigenfunction of the functional operator ψ_f . The trivial traveling pulse is unstable when the dominant eigenvalue of ψ_f is greater than 1.

The biomass in the equilibrium traveling wave depends on the specific functional forms of the harvesting function $g(n)$ and the recruitment function $f(n)$. However, the persistence of the population only depends on $g'(0)$ and $f'(0)$. In this paper, we only considered a proportional harvesting function, i.e. the amount of fish harvested obeyed $g(n) = (1 - h)n$. For this function, $g'(0) = 1 - h$. For the recruitment function we considered, $f'(0) = 1$.

A.2 Separable dispersal kernels It is not immediately obvious that the operator ψ will have any eigenfunctions. However, Jentzsch's theorem guarantees that there is an eigenfunction u , provided that the kernel k satisfies some properties [Zhou and Kot, 2011]. Finding the eigenfunctions and eigenvalues is in general a hard problem to solve. It becomes easier if the kernel k is separable, i.e., there are functions a_n, b_n such that $k(x - y) = \sum_{n=1}^{\infty} a_n(x)b_n(y)$. In that case, (5) becomes

$$\begin{aligned} \lambda u(x) &= R_0 g'(0) f'(0) \sum_{n=1}^{\infty} \left(a_n(x) \int_{-L/2}^{L/2} b_n(y - c) u(y) dy \right) \\ \Rightarrow \lambda \int_{-L/2}^{L/2} b_k(x - c) u(x) dx &= R_0 g'(0) f'(0) \sum_{n=1}^{\infty} \left(\int_{-L/2}^{L/2} b_n(x - c) u(x) dx \right) \left(\int_{-L/2}^{L/2} a_n(y) b_k(y - c) dy \right) \\ &\quad \text{for any } k \\ \Rightarrow \lambda d_k &= R_0 g'(0) f'(0) \sum_{n=1}^{\infty} A_{nk} d_n \end{aligned} \tag{6}$$

where

$$A_{nk} = \int_{-L/2}^{L/2} a_n(x) b_k(x - c) dx \text{ and } d_k = \int_{-L/2}^{L/2} b_k(x - c) u(x) dx$$

Finding the eigenvalues of (5) then reduces to finding the eigenvalues of the matrix comprised of entires $(A_{nk})_{n,k=1}^{\infty}$.

To find the equilibrium biomass, we rewrite (3) using the separable kernel as in Latore et al. [1998]:

$$\begin{aligned} n^*(x) &= \int_{-L/2}^{L/2} k(x + c - y) R_0 g(f(n^*(y))) dy \\ &= \int_{-L/2}^{L/2} \left(\sum_{n=1}^{\infty} a_n(x) b_n(y - c) \right) R_0 g(f(n^*(y))) dy \\ &= \sum_{n=1}^{\infty} a_n(x) \int_{-L/2}^{L/2} b_n(y - c) R_0 g(f(n^*(y))) dy \end{aligned}$$

If we define $m_n = \int_{-L/2}^{L/2} b_n(y - c) R_0 g(f(n^*(y))) dy$ then we find that

$$\begin{aligned} n^*(x) &= \sum_{n=1}^{\infty} m_n a_n(x) \text{ and} \\ m_n &= \int_{-L/2}^{L/2} b_n(y - c) R_0 g \left(f \left(\sum_{n=1}^{\infty} m_n a_n(y) \right) \right) dy \end{aligned} \tag{7}$$

The equations (7) allows us to find the m_n numerically and we then find the total equilibrium biomass by integrating $n^*(x)$ over space.

A.3 Gaussian dispersal kernel

The Gaussian dispersal kernel is given by

$$k(x - y) = \frac{1}{2\sqrt{D\pi}} e^{-\frac{(x-y)^2}{4D}},$$

where D is one half the variance of the kernel. This is a separable kernel with $a_n(x) = b_n(x) = \frac{1}{\sqrt{2n!\sqrt{D\pi}}} e^{-x^2/4D} \left(\frac{x}{\sqrt{2D}}\right)^n$ [Latore et al., 1998].

As a first approximation to k we ignore all but the 0th terms for a_n and b_n so that Equation (6) becomes

$$\begin{aligned} \lambda d_0(c) &= R_0(1-h)A_{00}(c)d_0(c) \\ \Rightarrow \lambda &= R_0(1-h)A_{00}(c) \\ \text{where } A_{00}(c) &= 2\sqrt{2} \exp\left(\frac{-c^2}{8D}\right) \left[\operatorname{erf}\left(\frac{L-c}{2\sqrt{2D}}\right) - \operatorname{erf}\left(\frac{-L-c}{2\sqrt{2D}}\right) \right] \end{aligned}$$

where erf is the error function. The critical rate of environmental shift c^* and the critical harvesting rate h^* are those values of c and h , respectively, that make $\lambda = 1$.

A.4 Sinusoidal dispersal kernel

The sinusoidal dispersal kernel is given by

$$k(x - y) = \begin{cases} \frac{w}{2} \cos(w(x - y)) & , |x - y| \leq \frac{\pi}{2w} \\ 0 & , |x - y| > \frac{\pi}{2w} \end{cases}$$

where L is the length of the patch and we assume $\frac{\pi}{2w} > L, c < \frac{\pi}{2w} - L$.

In this case, $k(x - y) = \frac{w}{2} \cos(wx) \cos(w(y - c)) + \frac{w}{2} \sin(wx) \sin(w(y - c))$ so that A_{ij} and d_i can be found for $i, j = 1, 2$ and (6) reduces to

$$\lambda^2 - \left(\frac{R_0(1-h)wL}{2} \cos(wc) \right) \lambda + \frac{R_0^2(1-h)^2}{16} (w^2L^2 - \sin^2(wL)) = 0.$$

If we solve for λ , we find

$$\lambda = (1-h)R_0 \left[\frac{wL \cos(wc)}{4} + \frac{1}{4} \sqrt{\sin^2(wL) - w^2L^2 \sin^2(wc)} \right].$$

Zhou and Kot [2011] solve for the critical speed, c^* , at which the population will be driven extinct:

$$c^* = c^*(R_0) = \frac{1}{w} \cos^{-1} \left[\frac{16 + R_0^2(1-h)^2(w^2L^2 - \sin^2(wL))}{8R_0(1-h)wL} \right].$$

In our model, we can additionally solve for the critical harvesting rate, h^* , at which the population will be driven extinct:

$$h^* = 1 - \frac{1}{R_0} \cdot \frac{4wL}{w^2L^2 - \sin^2(wL)} \left[\cos(wc) - \sqrt{\cos^2(wc) - 1 + \frac{\sin^2(wL)}{w^2L^2}} \right]$$

A.5 Approximate critical harvesting proportions

We will use the following Taylor series to make approximations of the critical harvesting proportions under the two dispersal kernels:

$$\begin{aligned}\cos(x) &= 1 - \frac{x^2}{2} \\ \cos^2(x) &= 1 - x^2 \\ \sin^2(x) &= x^2 - \frac{x^4}{3} \\ \operatorname{erf}(x) &= \frac{2}{\sqrt{\pi}} \left(x - \frac{x^3}{3} \right) \\ \exp(x) &= 1 + x + \frac{x^2}{2}\end{aligned}$$

For the Gaussian kernel we found

$$h^* = 1 - \frac{2\sqrt{2} \exp\left(\frac{c^2}{8D}\right)}{R_0 \left[\operatorname{erf}\left(\frac{L-c}{2\sqrt{2D}}\right) - \operatorname{erf}\left(\frac{-L-c}{2\sqrt{2D}}\right) \right]} \quad (8)$$

Using the Taylor series and the fact that $D = \frac{\sigma^2}{2}$ where σ^2 is the variance of the exponential kernel,

$$\begin{aligned}h^* &\sim 1 - \frac{\sqrt{2\pi} \left(1 + \frac{c^2}{8D} + \frac{c^4}{128D^2} \right)}{R_0 \sqrt{\pi} \left[\frac{L-c}{2\sqrt{2D}} - \frac{(L-c)^3}{3(2\sqrt{2D})^3} - \frac{-L-c}{2\sqrt{2D}} + \frac{(-L-c)^3}{3(2\sqrt{2D})^3} \right]} \\ &= 1 - \frac{1}{R_0} \cdot \frac{3\sqrt{2\pi}}{8L} \frac{(32\sigma^4 + 8c^2\sigma^2 + c^4)}{\sigma(12\sigma^2 - (L^2 + 3c^2))}\end{aligned}$$

For the sinusoidal kernel we found

$$h^* = 1 - \frac{1}{R_0} \cdot \frac{4wL}{w^2L^2 - \sin^2(wL)} \left[\cos(wc) - \sqrt{\cos^2(wc) - 1 + \frac{\sin^2(wL)}{w^2L^2}} \right] \quad (9)$$

Using the Taylor series and the fact that $w = \frac{\sqrt{\frac{\pi^2}{4}-2}}{\sigma}$ where σ^2 is the variance of the sinusoidal kernel,

$$\begin{aligned}h^* &\sim 1 - \frac{1}{R_0} \cdot \frac{12wL}{w^4L^4} \left[1 - \frac{w^2c^2}{2} - \sqrt{1 - w^2c^2 - \frac{w^2L^2}{3}} \right] \\ &= 1 - \frac{1}{R_0} \cdot \frac{4\sqrt{3}}{L^3(\pi^2-8)^{3/2}} \cdot \sigma \left[8\sqrt{3}\sigma^2 - (\pi^2-8)\sqrt{3}c^2 - 4\sigma\sqrt{12\sigma^2 - (\pi^2-8)(3c^2+L^2)} \right]\end{aligned}$$

In the case of both kernels, the critical harvesting proportion can be approximated by a function that looks like

$$h^* \sim 1 - \frac{1}{R_0} \cdot p(L)q(\sigma^2, c^2, L^2 + 3c^2) \quad (10)$$

where $p(L)$ is a decreasing function of the length of the viable patch L .

A.6 MPA fluctuations

After the simulations come to equilibrium, the fluctuations in total biomass per generation fluctuate more in MPAs that are larger and spaced farther apart than simulations in which the MPAs that are smaller and more closely spaced. The large MPAs have a slightly larger average population, however large MPAs here can induce fluctuations of biomass even in deterministic simulations. Thus we expect if reproduction was stochastic, large MPAs spaced far apart would be more likely to result in extinction of the population than more closely spaced, smaller MPAs.

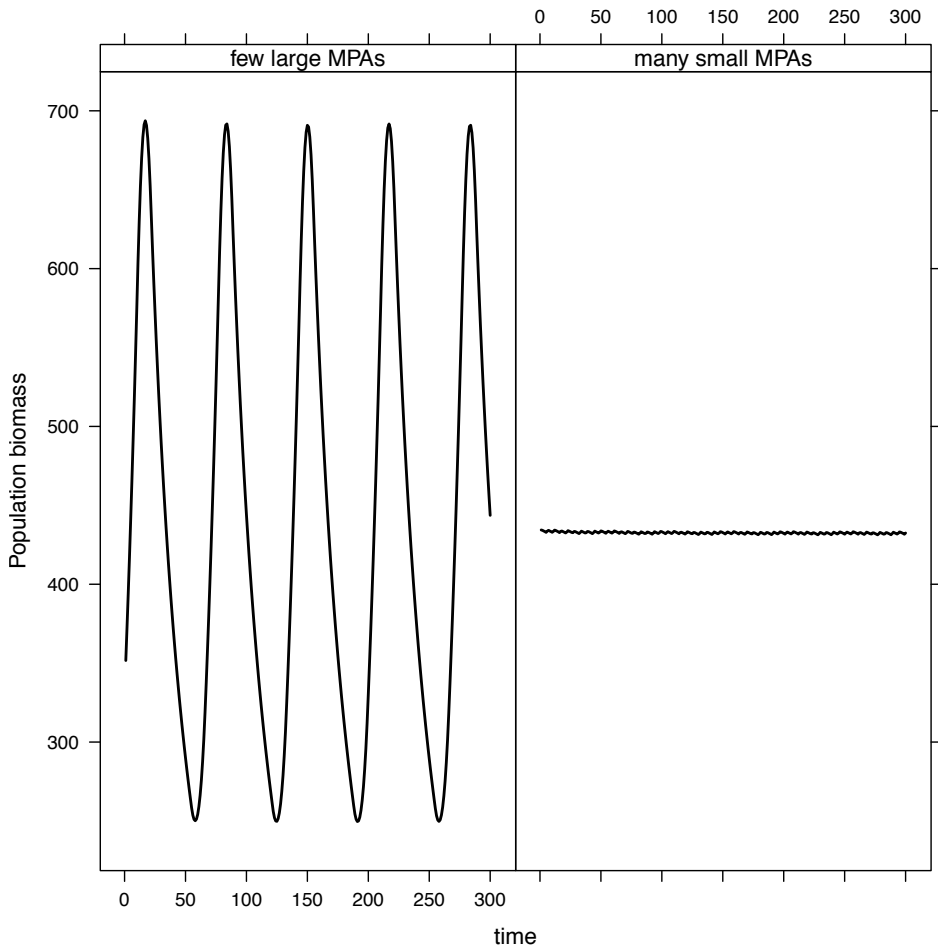


Figure 1: Total population biomass is on the y axis, and generation is on the x axis. These simulations were run with climate velocity = 0.1, and a proportional harvest rate = 0.08.

References

- J. Latore, P. Gould, and A. M. Mortimer. Spatial dynamics and critical patch size of annual plant populations. *Journal of Theoretical Biology*, 190(3):277–285, 1998.
- Ying Zhou and Mark Kot. Discrete-time growth-dispersal models with shifting species ranges. *Theoretical Ecology*, 4(1):13–25, 2 2011. ISSN 1874-1738. doi: 10.1007/s12080-010-0071-3.

```

#Laplace dispersal kernel
k<-function(x,y,b) return(1/2*b*exp(-b*abs(x-y)))

# dispersal matrix
d<-array(c(w,w))
#dispersal probabilities to point i from every point j
for(i in 1:w) d[i,]=k(world[i],world,b)

#Beverton-Holt recruitment
f<-function(n,R0,K) return(R0*n/(1+(R0-1)/K*n))

#Standard error removing NAs
stderr <- function(x) sqrt(var(x,na.rm=TRUE)/length(na.omit(x)))

moveMPA <- function(MPA.current = MPA.current, displaced =
displaced, mpa.yes=mpa.yes, mpa.no=mpa.no, world){

##### Move MPAS
# move MPA forward by <displaced> amount
next_MPA = MPA.current[displaced:length(MPA.current)]
lost <- MPA.current[1:(displaced-1)]

# are there any MPAs in <next_MPA>?
#any(test[[i]]$next_MPA==1)
# IF FALSE, then need to figure out how many 0s were lost in
# move, and make sure to preserve interval of zeros == mpa.no,
# then fill in mpa.yes,mpa.no to length of world. But also this
# is only for when mpa.no exists on both sides of MPA_next. If
# exactly to the edge of one reserve is lost, should shift down
# to next if statement
if(any(next_MPA==1)==FALSE & any(lost==1)==FALSE){
  # these are the intervals that are left behind as world moves
  # forward
  lost <- MPA.current[1:(displaced-1)]
  # this is the last continuous chunk of numbers at the end of
  # <lost>
  length_last <- rep(tail(rle(lost)$value,1),
    tail(rle(lost)$lengths,1))
  # want to know how long <length_last> is so can make sure to
  # get correct interval
}

```

```

L_int <- length(length_last)
# how many more zeros do we need before we start with mpa.yes
# again?
zero_add <- sum(mpa.no==0) - L_int - sum(next_MPA==0)
# this is what needs to be appended to <next_MPA>
new_MPA <- c(rep(0,zero_add),
             rep(c(mpa.yes,mpa.no),
                 length.out=length(world)))

}else{

# IF FALSE (there are some 1s) then we only care about the
# last interval of the <next_MPA>, is that protected or not?
last_step = tail(next_MPA,1)
# IF <last_step>==1
if(last_step ==1){
    #then how many 1s are at the end of the <next_MPA> section?
    end_step = rep(tail(rle(next_MPA)$value,1),
                   tail(rle(next_MPA)$lengths,1))
    # number of 1s at very end of lost interval
    # length of <end_step>
    end_int = length(end_step)
    # need to prepend sum(mpa.yes==1) - <end_step> to beginning
    prepend = rep(1, (sum(mpa.yes==1) - end_int))
    # and then fill out with mpa.no,mpa.yes for length of world
    fillOut <- rep(c(mpa.no, mpa.yes),
                  length = (length(world) - length(prepend)))
}else{
    # IF <last_step>==0
    end_step = rep(tail(rle(next_MPA)$value,1),
                   tail(rle(next_MPA)$lengths,1))
    # number of 0s at very end of lost interval
    # length of <end_step>
    end_int = length(end_step)
    # need to prepend sum(mpa.no==0) - <end_step> to beginning
    prepend = rep(0, (sum(mpa.no==0) - end_int))
    # and then fill out with mpa.no,mpa.yes for length of world
    fillOut <- rep(c(mpa.yes, mpa.no),
                  length = (length(world) ))
}

```

```

    new_MPA = c(prepend,fillOut)
}

MPA_finish = c(next_MPA,new_MPA)
MPA_finish = MPA_finish[1:length(world)]
# reduce to just the size of the world

return(MPA_finish)
}

m <- function(n, s, Fthresh = NA, Fharv = NA, mpa.yes = NA,
              mpa.no = NA, MPA.current=NA,effort_re_allocate=NA){
  # steps
  # 1. Harvest (check for thresholds, harvesting, MPA coverage)
  # 2. Patch moves (and MPAs are adjusted)
  # 3. Fish outside patch die
  # 4. Fish still alive (ie inside the patch) reproduce

  # harvesting occurs first - check to see how should
  # re-allocate effort

  if(!is.na(effort_re_allocate)){
    total_catch = sum(n)*Fharv
    available_total_pop = sum(n[which(MPA.current==0)])
    # pop with no MPA coverage
    available_fish = rep(0,length(n))
    available_fish[MPA.current==0] <-
      n[MPA.current==0]/available_total_pop
      # available_total_pop
      # proportion at each point
    catch_in_space <- total_catch*available_fish
    # allocate catch

    next_gen = n-catch_in_space
    next_gen[next_gen<0] = 0
  }else{
    if(!is.na(Fthresh)) { # if thresholds
      next_gen = ifelse(n < Fthresh,
                        n, n - (n - Fthresh) * Fharv)
    }
  }
}

```

```

if(!is.na(Fharv) & is.na(Fthresh)) {
  # if harvesting, no thresholds
  next_gen = n*(1-Fharv)
}
if(is.na(Fharv) & is.na(Fthresh)) {next_gen = n}
# if no harvesting of any kind

# but put fish back if places that were harvested were in
# the MPA
next_gen[MPA.current == 1] <- n[MPA.current == 1]
}

# move the patch
# calculate how far the patch will move through the population
# (if speed !=0)
displaced = ifelse(s>0,s/step_size,1)

# assign population that will still be inside the patch to
# moved patch
next_n = next_gen[displaced:length(next_gen)]

# fill in newly existing patch with 0s
next_n = c(next_n,rep(0,length.out=(displaced-1)))

# move MPAs?
if(s > 0){MPA_finish = moveMPA(MPA.current, displaced,
  mpa.yes,mpa.no,world)}else{MPA_finish= MPA.current}

# let patch reproduce
next_patch = vector(mode="numeric",length(world))

# keep individuals still in patch + those now in it due to
# move
next_patch[1:length(patch)] = next_n[1:length(patch)]

babies = next_patch*f_ind
n2 = babies %*% d *step_size
n2 = sapply(n2,f,R0,K)

MPA = MPA_finish

```

```

        return(list(n2,harv,MPA))
    }

longRun <- function(s, mpa.yes, mpa.no, Fthresh, Fharv, init,
                     MPA.start, generations_total, generations_av,
                     effort_re_allocate=NA){
  MPA.current <- MPA.start
  burn_in <- generations_total - generations_av
  for(t in 1:(burn_in)){
    output = m(n=init, s = s, Fthresh=Fthresh,Fharv=Fharv,
               mpa.yes = mpa.yes, mpa.no = mpa.no,
               MPA.current = MPA.current)
    init= output[[1]]
    MPA.current = output[[3]]
  }
  # make dataframe for simulation average
  pop <- rep(0,generations_av)
  for(keep in 1:generations_av){
    output = m(n=init, s = s, Fthresh=Fthresh,Fharv=Fharv,
               mpa.yes = mpa.yes, mpa.no = mpa.no,
               MPA.current = MPA.current)
    init = output[[1]]
    MPA.current = output[[3]]
    pop[keep] = sum(output[[1]])
  }
  # take mean for equil_abundance
  equil.pop = mean(pop)
  equil.sd = sd(pop)

  return(list(equil.pop,equil.sd))
}

# to introduce population to empty landscape, harvesting before
# adding speed treatment

startUp <- function(s, mpa.yes, mpa.no, Fthresh, Fharv, init,
                     MPA.start, burn_in,effort_re_allocate=NA){

```

```
MPA.current <- MPA.start
for(t in 1:(burn_in)){
  output = m(n=init, s = s, Fthresh=Fthresh, Fharv=Fharv,
  mpa.yes = mpa.yes, mpa.no = mpa.no,
  MPA.current = MPA.current)
  init= output[[1]]
  MPA.current = output[[3]]
}
return(list(init,MPA.current))
}
```

```

rm(list=ls())
setwd("/Users/efuller/Documents/Projects/Moving_fish/MovingFish/
Simluations/Aspatial_fast")
require(plyr)
require(lattice)

# load parameters, functions
source("Parameters.R")
source("Functions.R")

# set up different parameter combinations for all simulations

sims <- data.frame(model =
c("noThresh", "noThresh", "noThresh", "noThresh", "noThresh", "Thresh"),
MPA =
c("cons", "cons", "fish", "fish", "null", "null"),
effort_allocate = c(NA, TRUE, NA, TRUE, NA,
NA), stringsAsFactors=FALSE)

for(run in 1:nrow(sims)) {

# run analysis
# choose threshold or no threshold
model = sims$model[run] # "noThresh"; "Thresh"

# if no threshold, choose MPA: "null", "cons", "fish"
MPA = sims$MPA[run]
# choose how effort should be allocated if MPAs present.
effort_allocate = sims$effort_allocate[run]
effort_allocate = ifelse(MPA!="null", effort_allocate, NA)

# analysis
timed <- system.time(
  if(model=="noThresh")
{sapply(c("Parameters_nothresh.R", "Sim_noThresh.R"), source,,.GlobalE
nv)} else {
    if(model=="Thresh" & MPA == "null")
{sapply(c("Parameters_thresh.R", "Sim_thresh.R"), source,,.GlobalEnv)}
else {
      warning("model needs to be 'noThresh' or 'Thresh', MPA
}
}
}

```

```
needs to be 'null'")  
        }  
    }  
)  
  
cat(paste("Time elapsed: ",timed[1]/360," hours\n","Finished  
running a ", model, " simulation with ", MPA, " MPAs", " and effort  
re_allocate set to ", effort_allocate,".\n",nrow(sims)-run, "  
simulations left to go...",sep=""))  
}
```

```
# parameters for no-threshold simulations (just proportional
# harvesting)

# build dataframes
summaries <- data.frame(
  Equil.pop = rep(NA,length=length(speeds)*length(harvests)),
  Equil.sd = rep(NA,length=length(speeds)*length(harvests)),
  speed = rep(NA,length=length(speeds)*length(harvests)),
  harvest = rep(NA,length=length(speeds)*length(harvests)),
  thresh = rep(NA,length=length(speeds)*length(harvests))
)

# index for row number
rownumber <- matrix(seq(1:
(length(harvests)*length(speeds))),ncol=length(speeds))
```

```
# parameters for threshold simulations (no proportional harvesting)
harvests = 1
thresholds = seq(0,1,by=0.1)

# build dataframes
summaries <- data.frame(
  Equil.pop =
  rep(NA,length=length(speeds)*length(thresholds)),
  Equil.sd = rep(NA,
length=length(speeds)*length(thresholds)),
  speed = rep(NA,length=length(speeds)*length(thresholds)),
  harvest = rep(NA,length=length(speeds)*length(thresholds)),
  thresh=rep(NA,length=length(speeds)*length(thresholds)))

# index for row number
rownumber <- matrix(seq(1:
(length(thresholds)*length(speeds))),ncol=length(speeds))
```

```

#####
## Parameters & Building Structures ##
#####

step_size=0.01 #distance between points in space
b=.5 #parameter for Laplace dispersal kernel
R0=5 #growth parameter for recruitment
K=100 #carrying capacity parameter for juvenile density dependence
threshold = 0.001 #difference between generation populations.
burn_in = 2000 # number of generations to run simulations before
               checking for equilibrium conditions
speeds = seq(0,.5,by=0.02)
harvests = seq(0,.2,by=0.01)
f_ind = 1 #per capita reproductive rate
generations_total = 8000
generations_av = 2000

patch = seq(0,1,by=step_size)
world = seq(-.51,4.5, by = step_size) # to run the MPA versions,
                                         world has to be at least 400 steps (max distance between MPAs in
                                         "cons" run)
w = length(world)

cons.yes = rep(1,4*b/step_size)
cons.no = rep(0,8*b/step_size)
fish.yes = rep(1,floor((1/3*b)/step_size)) # had to round because
                                              not complete step size. Rounded down.
fish.no = rep(0,floor((2/3*b)/step_size))

null.yes = rep(0,length(world))
null.no = rep(0, length(world))

move_window = 100

```

```

# set MPAs
if(MPA=="cons") {mpa.yes=cons.yes; mpa.no=cons.no} else {
  if(MPA=="fish") {mpa.yes=fish.yes; mpa.no=fish.no} else {
    if(MPA=="null") {mpa.yes=null.yes; mpa.no=null.no} else{
      if(exists("MPA")) warning(paste("MPA needs to be
'cons', 'fish', or 'null'.",sep=""))
    }
  }
}

# initializing the population with no pressure (no harvesting, no
climate)
init<-rep(0,w) # rows are world, columns are time
init[which(patch==0.55)]=50
MPA.start = rep(c(mpa.yes,mpa.no),length.out=length(world))

output <-
startUp(s=0,mpa.yes=mpa.yes,mpa.no=mpa.no,burn_in=burn_in,
Fharv=NA, Fthresh=NA, init=init, MPA.start = MPA.start)
init.s <- output[[1]]
MPA.start <- output[[2]]

for(q in 1:length(speeds)){
  for(j in 1:length(harvests)){
    # adding harvesting
    output <-
startUp(s=0,mpa.yes=mpa.yes,mpa.no=mpa.no,burn_in=burn_in,Fharv=har
vests[j],Fthresh=NA, init=init.s, MPA.start = MPA.start,
effort_re_allocate=effort_allocate)
    init.h <- output[[1]]
    MPA.start <- output[[2]]

    # adding speed
    output <- longRun(s=speeds[q], mpa.yes=mpa.yes,
mpa.no=mpa.no, Fthresh=NA, Fharv=harvests[j], init = init.h,
MPA.start = MPA.start, generations_total=generations_total,
generations_av=generations_av, effort_re_allocate=effort_allocate)

    # save output
    pop = output[[1]]
  }
}

```

```
pop.sd = output[[2]]
summaries[rownumber[j,q],] <- c(pop, pop.sd, speeds[q],
harvests[j], ifelse(exists("Fthresh"), Fthresh, NA))
}

write.csv(summaries,file = paste("Data/
MPA",MPA,"_",Sys.Date(),".csv",sep=""))
```

```

# initializing the population with no pressure (no harvesting, no
climate)
  init<-rep(0,w) # rows are world, columns are time
  init[which(patch==0.55)]=50
  MPA.start = rep(c(mpa.yes,mpa.no),length.out=length(world))

  output <-
startUp(s=0,mpa.yes=mpa.yes,mpa.no=mpa.no,burn_in=burn_in,
Fharv=NA, Fthresh=NA, init=init, MPA.start = MPA.start)
  init.s <- output[[1]]
  MPA.start <- output[[2]]

for(q in 1:length(speeds)){
  for(j in 1:length(thresholds)){
    # adding harvesting
    output <-
startUp(s=0,mpa.yes=mpa.yes,mpa.no=mpa.no,burn_in=burn_in,Fharv=1,F
thresh=thresholds[j], init=init.s, MPA.start = MPA.start,
effort_re_allocate=effort_allocate)
    init.h <- output[[1]]
    MPA.start <- output[[2]] Fharv=1

    # adding speed
    output <- longRun(s=speeds[q], mpa.yes=mpa.yes,
mpa.no=mpa.no, Fthresh=thresholds[j], Fharv=1, init = init.h,
MPA.start = MPA.start, generations_total=generations_total,
generations_av=generations_av, effort_re_allocate=effort_allocate)

    # save output
    pop = output[[1]]
    pop.sd = output[[2]]
    summaries[rownumber[j,q],] <- c(pop, pop.sd, speeds[q],
1, ifelse(exists("thresholds"), thresholds[j],NA))
  }
}

write.csv(summaries,file = paste("Data/
Thresh_",Sys.Date(),".csv",sep=""))

```